buildings

MDPI

Article

Parameter Selection for the Dehumidification System of the Main Cable of Suspension Bridge Based on Ventilation Experiments

Zhihang Guo [1], Wenhao Sui [1], Hua Guan [2], Pei Peng [1], Qun Liu [1] and Jianzhong Shi [1,*]

[1] School of Environmental Engineering, Wuhan Textile University, Wuhan 430200, China; guozhihang521@foxmail.com (Z.G.); suiwenhao7@live.com (W.S.); ppeng@wtu.edu.cn (P.P.); mrliuqun@outlook.com (Q.L.)

[2] Zhejiang Zhoushan Cross-Sea Bridge Co., Ltd., Ningbo 316034, China; gh_1983@hotmail.com

* Correspondence: 1990011@wtu.edu.cn; Tel.: +86-159-0274-0655

Highlights:

What are the main findings?

- Ventilation experiment of the main cable of the suspension bridge during the operation period.

What is the implication of the main finding?

- The parameter design of the dehumidification system is guided by the ventilation experiment data.

Abstract: Moisture in the main cable is the main cause of steel wire corrosion. Modern suspension bridges utilize main cable dehumidification systems to prevent corrosion. The main cable ventilation experiment can help the selection of the system parameters. This research is based on the ventilation experiment of the main cable of Xihoumen Bridge to obtain the design parameters of the dehumidification system. According to the experiment, the suitable dehumidification distance is 150–180 m; the pressure loss of the main cable with a length of 150 m is 200–300 Pa, so the inlet pressure should be higher than 300 Pa; increasing the outlet clamp can increase the dehumidification efficiency; Under single inlet and double outlet situation, every 100% increase in air volume increases the dehumidification capacity is about 35%. The water content of the main cable of Xihoumen Bridge is 5.74 kg/m^3, and 1 m^3 of dry air can remove 5.5 g of water under experimental conditions, and the minimum air volume is 30 m^3/h. The main factors affecting the dehumidification time are air volume and leakage rate. Input these parameters into the dehumidification system for the dehumidification experiment, and the water content of the outlet clamp will drop by about 37.5% within ten days.

Keywords: suspension bridge; dehumidification system; main cable; ventilation experiments; anti-corrosion system

check for updates

Citation: Guo, Z.; Sui, W.; Guan, H.; Peng, P.; Liu, Q.; Shi, J. Parameter Selection for the Dehumidification System of the Main Cable of Suspension Bridge Based on Ventilation Experiments. *Buildings* **2023**, *13*, 1386. https://doi.org/10.3390/buildings13061386

Academic Editors: Chong Zhang, Rui Guo, Yunran Min and Chaoqun Zhuang

Received: 28 April 2023
Revised: 20 May 2023
Accepted: 25 May 2023
Published: 26 May 2023

1. Introduction

The Menai Suspension Bridge in England is the earliest created suspension bridge in the world. It was built in 1826 and has a main span of 577 feet [1]. It is the first large-scale suspension bridge in the world. Since then, many famous suspension bridges have been built around the world, such as the Brooklyn Bridge in New York City, the Golden Gate Bridge in San Francisco, and the Akashi Kaikyo Bridge in Japan. Suspension bridge designs have a service life of over 100 years. Many efforts have been made to ensure the safety of suspension bridges. Fakhimi et al. provided an effective heuristic solution method based on an exact solution to the MILO problem through model analysis and computational experiments [2]. Suspension bridges are subjected to loads from various aspects for a long time during operation, and Ghyabi et al. proposed a method for quantifying bridge deformation based on vision [3]. The main cable is the main force-bearing structure of the suspension bridge, which determines the operation safety of the suspension bridge [4]. The main construction material of the main cable is steel, and its greatest threat during operation is corrosion [5]. Moisture in the main cable is the main cause of its corrosion [6]. When the ambient humidity is higher than 60%, the corrosion rate of steel will be significantly accelerated. The accelerated corrosion experiments conducted by Suzumura and Nakamura [7,8] show that under the condition of 100% relative humidity, the life index of the main cable steel wire is only 34 years. In order to prevent corrosion of the main cable, people install a protective layer on the outside of the main cable to isolate the moisture in the external environment and other media that cause corrosion, so as to protect the internal environment of the main cable. However, there is a gap of several months between the erection of the main cable and the installation of the passive anti-corrosion system for the main cable. During this period, rainwater invades and accumulates inside the main cable, still causing corrosion. The coating wrapped around the outside of the main cable will crack as it ages over time, causing the protective putty wrapped inside to be completely exposed to the air. As the weather changes, the physical and chemical properties of the protective putty change, and its anti-corrosion effect on the main cable also disappears. Traditional anti-corrosion technology can only delay the speed of corrosion to a certain extent and cannot prevent corrosion from occurring. Nowadays, people use dry air to dehumidify the main cable wire to prevent corrosion [9,10]. This method was first used on the Akashi Kaikyo Bridge [11]. The main cable dehumidification system uses dry air prepared by a dehumidifier as a desiccant [12]. After cooling and pressurization, it enters the interior of the main cable steel wire from an air clamp. After absorbing a certain amount of moisture, it is discharged to the atmospheric environment or flows to the inlet of the dehumidifier through another air clamp for dehumidification before entering the next dehumidification process [6,11,13].

When using dry air to protect the main cable, Air flows radially into the main cable at the air inlet clamp, then flows axially, and finally flows radially out of the main cable at the outlet clamp. Dry air absorbs moisture in the main cable while flowing, drying, and dehumidifying the internal environment of the main cable. After a certain period of time, the relative humidity of the internal environment of the main cable can be kept below 60% [14,15], so that the steel wire inside the main cable does not have the conditions for rusting and will not corrode, thereby protecting the main cable [8,16].

The design of the main cable dehumidification system involves many parameters [13], mainly including: internal water content of the main cable, pressure loss, air volume, pressure, dehumidification time, and dehumidification distance, and there is a complex relationship between these parameters. Excessive intake pressure will cause the outer layer of the main cable to be subject to circumferential expansion force, which may damage the outer layer of the main cable. Cao et al. tested the circumferential expansion performance of the outer winding system of the main cable of the suspension bridge [17]. Chen et al. proposed the design of an air supply inside the main cable [18]. This design installs the air supply pipe inside the main cable, but it is not suitable for the suspension bridge that has been built. Also, Wei Chen et al. studied the internal resistance loss of the air supply pipeline [19]. Wei et al. treated the complex flow of fluid inside the main cable as the flow in a circular pipe of equivalent diameter [20]. Peng et al. found that the air flow and dehumidification time in the main cable are directly proportional to the supply air flow, and inversely proportional to the supply air length and leakage rate [13]. On the basis of experiments, Jia et al. obtained the empirical formula of the dry air mass transfer coefficient [21]. These studies provide a reference for the design of the dehumidification system of the main cable of the suspension bridge, but the conditions of different suspension bridges are inconsistent.

The main cable ventilation experiment can help us to select these parameters [22,23]. The Xihoumen Bridge has been built for more than ten years. In order to ensure its safe operation, it was decided to install a dehumidification system for the main cable. As the main cable length, service life and actual operating conditions of each suspension bridge are different, there is no similar dehumidification system design available for reference. The design team had to find a way to guide the design of the main cable dehumidification system. Recently, the first ventilation experiment of suspension bridge main cables during the operation was conducted on Humen Bridge. Through experiments, the researchers found that the outer layer of the main cable of the Humen Bridge had serious leakage, and the interior was full of corrosion, so the dehumidification system had to use higher pressure and air volume. It has also been found that increasing the number of vents facilitates the drainage of moisture. The design team wants to use the previous experience of the Humen Bridge to conduct ventilation experiments on the main cable of the Xihoumen Bridge. Based on the experiments, the team will be guided in the design of the dehumidification system. Based on the main cable ventilation experiment of Xihoumen Bridge, this study selects the appropriate inlet pressure, air volume and dehumidification distance for the dehumidification system of the main cable. Estimate the dehumidification time by calculating the water content inside the main cable, the dehumidification capacity of dry air and the leakage rate.

2. Materials and Methods

2.1. Introduction to the Xihoumen Bridge

The Xihoumen Bridge, located in Zhoushan City, Zhejiang Province, China, is a critical component of the Zhoushan Cross-Sea Bridge project. This bridge has been in operation for over a decade, thus our measurements should be ensured the health and safety of the bridge's main cable when installing a dehumidification system. In order to obtain more detailed data on the internal ventilation conditions of the main cable, an initial ventilation and dehumidification experiment was conducted on the main cable section to determine its internal resistance characteristics. The experimental results were used as a basis for designing the main cable dehumidification system.

2.2. Introduction to Ventilation Experiments

The ultimate goal of the ventilation experiment is to design the parameters for the main cable dehumidification system. The parameters that need to be determined include: dehumidification distance, air inlet pressure, air volume, air leakage rate, and the optimal air supply mode. By changing the distance between the air inlet and outlet while keeping other conditions constant, the optimal dehumidification distance for that main cable section can be determined. By changing the air inlet pressure while keeping other conditions constant, the optimal air supply pressure and air volume under those conditions can be determined. The air leakage rate of the main cable can be inferred from the difference in flow rate between the air inlet and outlet.

2.3. Ventilation Experiment Arrangement

2.3.1. Selection of Experimental Section and Equipment Layout

Due to the considerable length of the main cable, conducting ventilation experiments along its entire length presents significant challenges and incurs high costs. As such, the lowest point in the middle of the main cable is typically selected for ease of construction and installation of experimental equipment.

In the selection of the experimental distance, the experimenters referred to many suspension bridges that have been installed with dehumidification systems. The dehumidification distance of some suspension bridges is shown in Table 1.

Table 1. Dehumidification distance of some suspension bridges in China.

Name	Main Span	Dehumidification Distance
Jiangyin Yangtze River Bridge	1385 m	170 m
Runyang Bridge	1490 m	210 m
Qingshui River Bridge	1130 m	200 m
Yangsigang Yangtze River Bridge	1700 m	150~200 m
Longjiang suspension bridge	1196 m	200 m
Jin'an Jinsha River Bridge	1386 m	150~200 m

Based on the dehumidification distance used by previously implemented main cable dehumidification systems, a total length of 396 m at the lowest point of the Xihoumen Bridge main cable span was selected as the experimental section. Within this section, experimental distances of 90 m, 72 m, 54 m, and 36 m were chosen and tested using different distance combinations. The layout of the experimental section is shown in Figure 1.

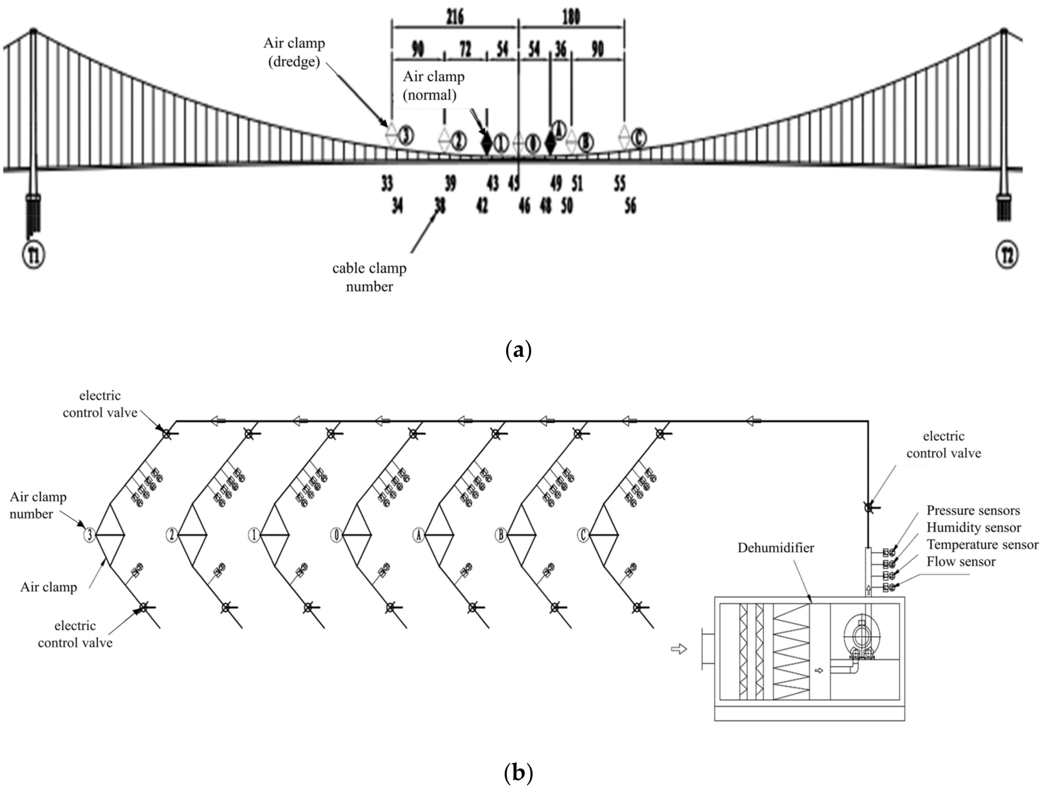

Figure 1. (**a**) General layout of main cable ventilation experiment; (**b**) Layout of main cable ventilation experiment equipment.

2.3.2. Experiment Equipment

(1) Rotary dehumidification

Figure 2 shows the rotary dehumidifier used in the experiment. Rotary wheel dehumidifier is the most commonly used dehumidification equipment in the suspension bridge dehumidification system at present. Its dehumidification principle is mainly physical adsorption. When the external air passes through the non-stop rotating dehumidification wheel, the water vapor in the air is absorbed by the porous honeycomb in the dehumidification wheel. The shape of the adsorbent material is adsorbed, and the air humidity is reduced. When the rotating dehumidification wheel passes through the regeneration area of the dehumidifier, it is heated so that the adsorbed moisture becomes water vapor again and is discharged. Table 2 shows the relevant parameters of the rotary dehumidifier.

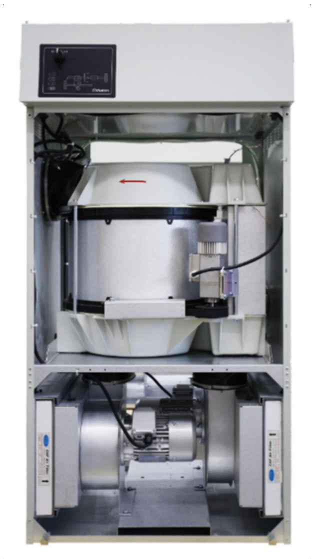

Figure 2. Rotary dehumidifier.

Table 2. Parameters of the rotary dehumidifier.

Index	Require	Remark
Rated dehumidification capacity	≥6 kg/h	At 20 °C, humidity 80%
Rated energy efficiency	≤1.4 KW/kg	At 20 °C, humidity 80%
Rated air volume	690 Nm^3/h	
Dew point temperature	≤−5 °C	
Regeneration temperature	100~150 °C	
Power supply system	TN-S	
Power supply frequency	50 Hz	

(2) High pressure fan

Figure 3 shows the high-pressure blower used in the experiment. In the experimental system, a high-pressure fan is required to provide pressure and send air into the interior of the main cable. Since the experiment needs to obtain data on different inlet pressures, the high-pressure fan needs a larger adjustment range. Its related parameters are shown in Table 3.

Figure 3. High pressure fan.

Table 3. Parameters of high-pressure fan.

Index	Require
Fan type	Centrifugal
Motor type	Induction motor
Number of motor phases	Three phase
Power factor	≥0.85
Rated voltage	380 V AC
Power supply frequency	50 Hz

(3) Pressure sensor

Figure 4 shows the pressure sensor used in the experiment. During the experiment, it is necessary to monitor the internal pressure of the main cable inlet and outlet clamps to adjust the inlet pressure and obtain pressure data related to other positions. The pressure sensor parameters are shown in Table 4.

Figure 4. Pressure sensor.

Table 4. Parameters of the pressure sensor.

Index	Require
Range	0~10 kPa
Precision	0.25% FS
Power supply	24 V DC
Degree of protection	IP65
Operating temperature range	−40~85 °C
Installation method	Threaded installation

(4) Flow rate sensor

Since the experimental system uses a DN50 pipe as the air supply pipe, the diameter is small and there is no suitable area to install a flow sensor, a flow rate sensor is used to obtain the internal flow rate of the pipe, and the corresponding air volume is obtained through conversion. This method replaces the flow sensor. Figure 5 shows the flow rate sensor used in the experiment. The relevant parameters are shown in Table 5.

Figure 5. Flow rate sensor.

Table 5. Parameters of flow rate sensor.

Index	Require
Range	0~30 m/s
Precision	0.1 m/s
Power supply	24 V DC
Degree of protection	IP65

(5) Humidity Sensor

Figure 6 shows the humidity sensor used in the experiment, and its parameters are shown in Table 6.

Figure 6. Humidity sensor.

Table 6. Parameters of the humidity sensor.

Index	Require
Range	0~100% RH
Precision	1%
Power supply	24 V DC
Degree of protection	IP65

(6) Installation of some experimental equipment

The specific installation of some experimental equipment are shown in Figure 7.

2.4. Experimental Procedure

The Xihoumen main cable ventilation experiment is divided into three parts.

2.4.1. On-Off Experiment

An inspection of the main cable of the Xihoumen Bridge revealed that its interior was filled with corrosion products and had poor ventilation conditions. Prior to the formal experiment, an on-off experiment was conducted to evaluate the gas flow conditions inside the main cable. A total of 7 air clamps were installed in the experimental section, numbered 3, 2, 1, 0, A, B, and C. Among them, air clamps A and 1 were not equipped with guide plates. Before the experiment, air was supplied to each air clamp separately to ensure that the air clamp could be ventilated. With the air supply flow rate kept constant, air was supplied to each air clamp and the pressure of the air clamp was monitored. The on-off experiment can also determine whether this conduction method can improve gas flow conditions and thereby enhance the dehumidification effect of the main cable. Figure 8 shows the guide plate installation process.

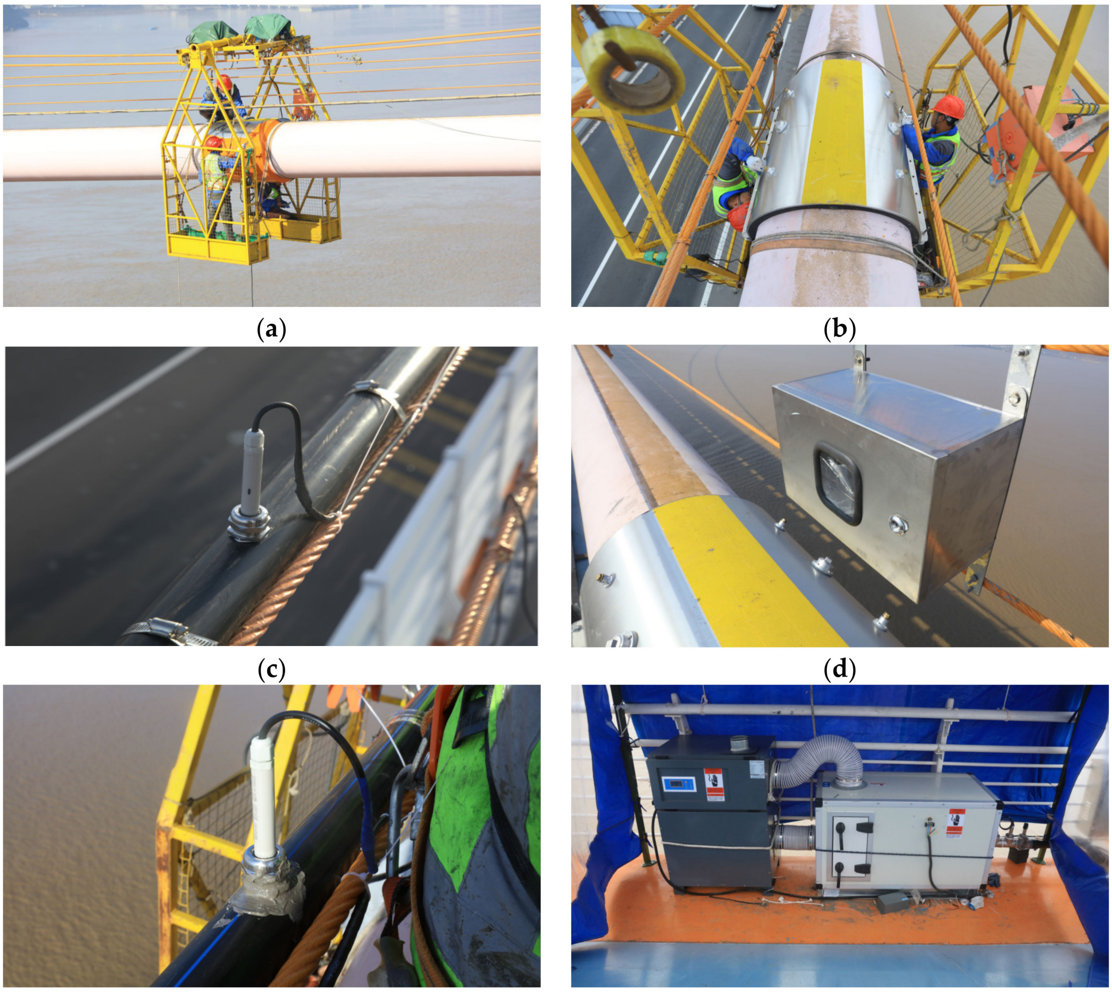

(**a**) (**b**) (**c**) (**d**) (**e**) (**f**)

Figure 7. (**a**) Installation of air clamp and pipeline; (**b**) Installation of air clamp and pipeline; (**c**) Sensor installation; (**d**) Installation of monitoring equipment; (**e**) Sensor installation; (**f**) Ventilation experiment dehumidifier installation.

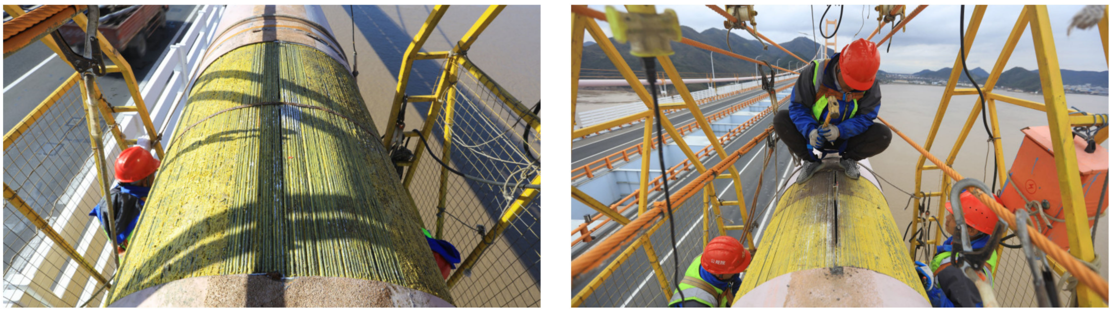

(**a**) (**b**)

Figure 8. (**a**) Main cable with outer protective layer removed; (**b**) Install the guide plate.

2.4.2. Ventilation Experiment

Within a total length of 396 m of the main cable section, seven air clamps were installed. One or more air clamps were selected as inlet clamps and one or more air clamps as outlet clamps. Different positive pressures were applied at the inlet clamps and the gas flow rate, temperature and humidity at the inlet and outlet clamps were monitored and recorded. Each combination of inlet and outlet became a working condition, and different inlet pressures were tested under each working condition. After the sensor readings stabilized for a period of time, data was recorded. The entire ventilation experiment had a total of 20 working conditions.

2.4.3. Dehumidification Experiment

Dehumidification experiment Based on the parameters of the dehumidification system obtained from the analysis of data collected from ventilation experiments, overall dehumidification was carried out in the main cable experimental section by simulating the operation of the main cable dehumidification system. Dry air was introduced into the main cable and data on gas at inlet and outlet clamps was recorded. After prolonged dehumidification, the internal environment of the main cable was reduced to a humidity level where steel wire corrosion is unlikely to occur. The dehumidification rate of the main cable dehumidification system was estimated, and it was possible to understand the correlation between weather data and operating conditions of the dehumidification system which is helpful for guiding operation after commissioning.

3. Results

3.1. On-Off Experiment

Air clamps 3, 2, 1, 0, A, B, and C were opened separately as inlet clamps while all remaining air clamps were closed when a single air clamp was opened. The impact of installing guide vanes on dehumidification system intake efficiency was evaluated by detecting pressure data at that air clamp. Test data is shown in Table 7.

Table 7. Pressure gauges of each air clamp for the on–off test.

Inlet	Pressure (Pa)						
	C	B	A	0	1	2	3
C	523	204	52	5	0	0	0
B	230	703	208	58	10	0	20
A	25	223	1282	103	29	0	21
0	12	78	195	1038	286	13	16
1	0	10	25	226	1941	120	34
2	0	0	0	23	148	921	98
3	0	0	0	0	9	34	936

During the experiment, the dehumidifier maintained its maximum outlet power. The results showed that at the same air clamp, the pressure of the A and 1 air clamps without the guide plate installed was significantly higher than that of the air clamps with the guide plate installed. After peeling off the outer protective layer of the main cable, it was found that the inner steel wire was filled with protective putty that was difficult to remove, which prevented dry air from entering the main cable. The function of the guide plate is to pry open a gap for the steel wire, so that the dry air can be easily sent into the main cable without destroying the stress structure of the steel wire. The experimental results show that the installation of the guide plate has a positive effect on the dry air entering the main cable.

3.2. Ventilation Experiment

First, test the single inlet and outlet conditions. According to different combinations of inlet and outlet air clamps, multiple dehumidification distances can be obtained. Select working conditions with dehumidification distances of 90, 216, 306, and 396 m. Run the dehumidifier at maximum power and perform inlet and outlet air tests during these working conditions. The results are shown in Table 8. It was found that when the dehumidification distance was above 306 m, no outlet data could be detected by the outlet clamp. When the dehumidification distance was 306 m, a weak airflow could be detected by the outlet clamp. At this time, the outlet ratio was below 5%, and the dehumidification effect was not ideal. Therefore, the best experimental distance is between 90~216 m.

Table 8. Discharge ratio of dehumidification distance under partial conditions.

Inlet	Outlet	Maximum Dehumidification Distance (m)	Discharge Ratio (%)
3	2	90	15.05
3	0	216	8.602
3	B	306	4.301
3	C	396	0

The shorter the dehumidification distance under the same air volume, the better the inlet and outlet effect. The results of the single supply and outlet indicate the gas flow status inside the main cable of the Xihoumen Bridge. Judging from the experimental data, when the supply air distance reaches more than 200 m, the discharge ratio is extremely low and the gas has been lost before reaching the outlet clamp. The parameters for selecting the dehumidification distance can refer to single inlet and outlet results, that is, it should not exceed 200 m, and a higher dehumidification effect can be obtained between 150 m and 180 m.

Next, analyze single inlet and double outlet conditions. Choose working condition 1 (2 inlet, 3 and 0 outlets); working condition 2 (0 inlet and 2 and B outlets) for two experimental conditions. The experimental results and fitting curves are shown in Figures 9 and 10.

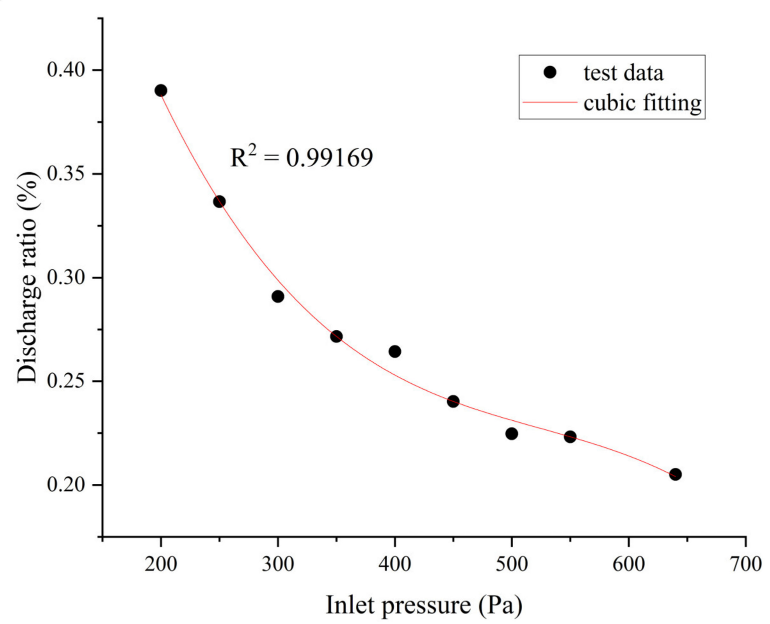

Figure 9. Test data and fitting results of condition 1.

The experimental data of single inlet and double outlet presents a certain regularity. By fitting the experimental data with a curve, the best fit to the measured data is achieved when the fitting function is a cubic polynomial function. At low pressure, a higher discharge ratio can be obtained, but due to the small air volume, the amount of gas discharged is small, the amount of water that can be discharged is less, and the corresponding dehumidification time will increase. The discharge ratio of both working conditions decreases rapidly when the inlet pressure is 200~400 Pa; the discharge ratio tends to be stable when the inlet pressure is 400~750 Pa. When the pressure exceeds a certain value, the change in the discharge ratio brought about by continuing to increase the pressure is not obvious.

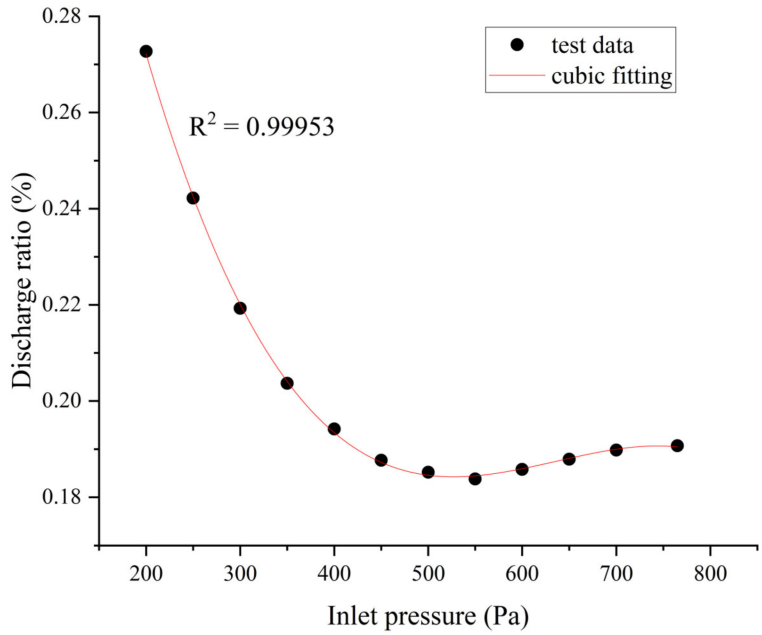

Figure 10. Test data and fitting results of condition 2.

To analyze the change in dehumidification benefits brought about by increasing air volume, the inlet air volume and outlet ratio at 200 Pa are used as baseline values, and data at other pressures are used as changes, as shown in Figure 11.

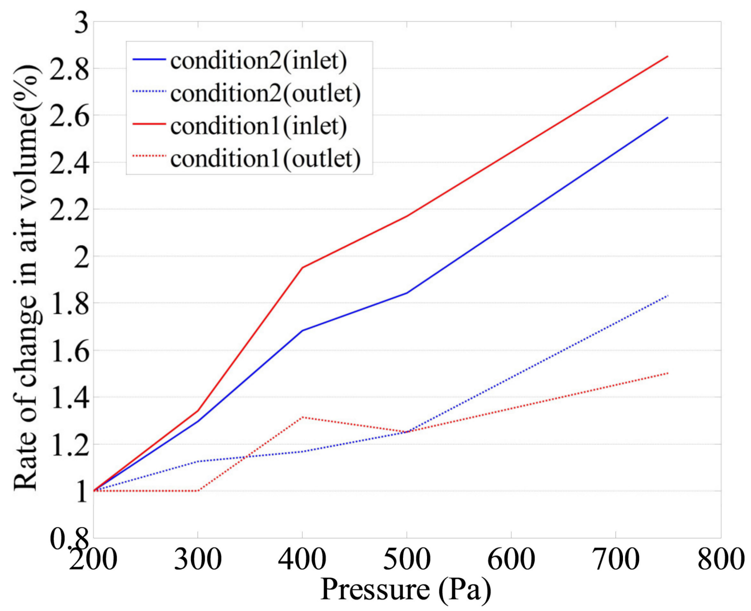

Figure 11. The rate of change in air volume varies with pressure.

The change in outlet air volume varies with the change in inlet air volume. The overall trend is consistent, but the slope k(Change rate of air volume at inlet and outlet) of the line segment is different. The increase rate of the outlet is obviously lower than that of the inlet. In working condition 1, when the inlet pressure increases from 200 Pa to 300 Pa, there is no change at the outlet end, and even a downward trend appears when the inlet pressure increases from 400 Pa to 500 Pa. In working condition 2, although there was no decline during the process of increasing pressure from 200 Pa to 500 Pa, the growth rate was lower than that of inlet pressure above 500 Pa.

To explore the impact of increasing outlet clamps on dehumidification effects, a single air inlet, and four air outlet conditions were also performed. The change of outlet ratio with pressure and fitting curve is shown in Figure 12.

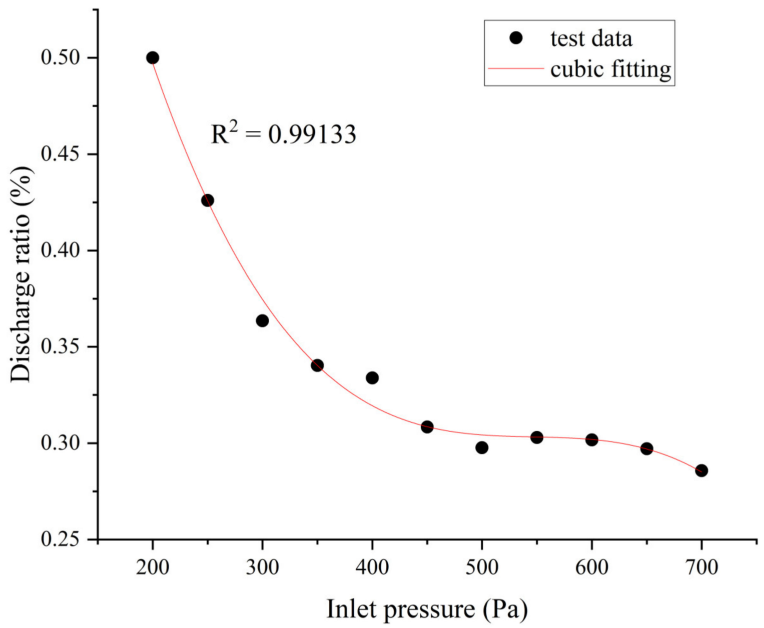

Figure 12. Test data and fitting results.

The residual values of both single-inlet four-outlet and single-inlet double-outlet fitting functions are smallest when they are cubic polynomials, and their fitting curves are closest to the original data. The regularity shown by the single-inlet four-outlet experiment is similar to that of the single-inlet double-outlet experiment. The difference is that the multi-outlet overall discharge ratio is higher and increasing the number of outlet clamps can improve the discharge ratio. Similarly, taking inlet and outlet air volume at 200 Pa as baseline value and plotting changes in air volume at other pressures as shown in Figure 13.

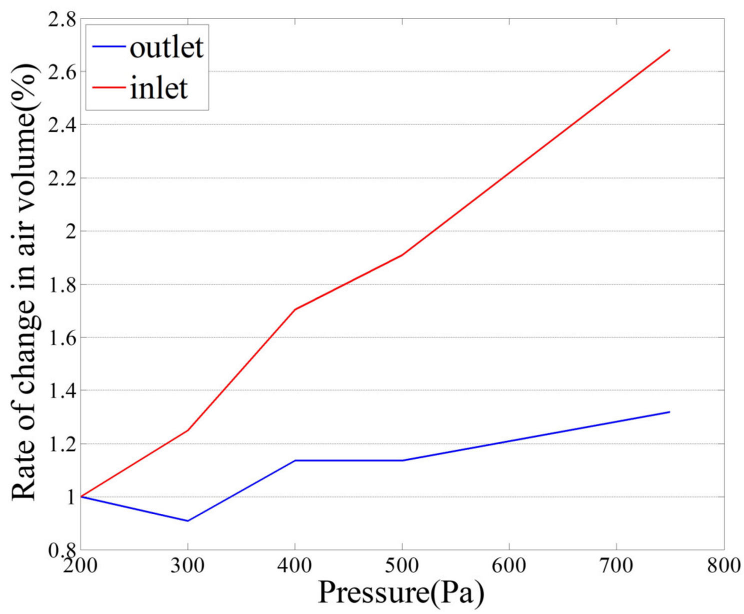

Figure 13. The rate of change in air volume varies with pressure.

Compared with the data of double discharge, the outlet benefit brought by increasing the inlet air volume of a single inlet and four discharge is lower than that of double discharge. In double discharge, an increase in outlet up to 120% requires an increase in inlet up to 160% of the baseline, while four discharge requires approximately 220% of the baseline value for the inlet to increase by 20% of the discharge. Multiple outlet clamps improve the discharge ratio, but each outlet clamp dilutes the effect brought about by increasing inlet pressure when increasing inlet pressure. To improve the outlet volume of multi-outlet, greater inlet pressure, and air volume are required.

4. Discussion

4.1. Water Content in the Main Cable

The water content in the main cable is important data for calculating the drying time and air volume. There are mainly two sources of water in the main cable. One is due to the long construction process, which is easily affected by factors such as rainfall, and water remaining inside. The second is the dynamic load during the use of the main cable, aging, and damage of the outer protective layer, causing water vapor in the air and rainwater to invade on rainy days [24]. The water content in the main cable is difficult to measure. According to a test result from Jiangsu Provincial Transportation Planning and Design Institute, for parts where the angle between the tangent of the suspension line of the main cable and the horizontal direction is within 0~11°, the water content is calculated as 7.5%, and other parts of the main cable The water content is calculated as 5%. When estimating the actual water content of the main cable, 5~7.5% can be selected according to the actual steel wire laying conditions inside the main cable.

The pores in the main cable are generated by stacking thousands of steel wires. The porosity can be calculated by the cross-sectional area inside the main cable, steel wire diameter, and steel wire quantity [13].

$$\varepsilon = \frac{S_1}{\pi {r_0}^2 I} \tag{1}$$

where ε is the internal porosity of the main cable, S_1 is main cable cross-sectional area, r_0 is wire radius, I is the number of wires.

Generally, the porosity of main cables is around 20% (However, the porosity will change with different bending angles of the main cable, and the temperature change will cause the thermal expansion and contraction of the steel wire to also affect the porosity. 20% here is an estimate). Water occupies 5% of the pores in the main cable [20]. The amount of water contained in the main cable segment of length L is:

$$W = 0.05 \varepsilon L \pi r^2 \tag{2}$$

where W is the amount of water contained in the main cable, ε is the internal porosity of the main cable.

According to the data of the main cable of Xihoumen Bridge, the water content of the main cable is 5%, and the water content inside the main cable of Xihoumen Bridge is calculated as 5.74 kg/m^3.

4.2. Pressure Loss and Inlet Pressure

The key issue of main cable dehumidification is the problem of air flow and heat and mass exchange. The theory involved in this kind of air flow and heat and mass exchange problem in a narrow space is complex. In order to facilitate analysis and calculation, some simplifications are made to the problem according to actual conditions.

Air flows from the main cable air inlet clamp to the outlet clamp. According to an experimental report by Jiangsu Provincial Transportation Planning and Design Institute, the pressure change during this flow process generally does not exceed 3%. (Based on the experimental data of Humen Bridge and Runyang Bridge), with the purpose of protecting the outer protective layer of the main cable. Therefore, the pressure change during air flow in the main cable cannot exceed 4% [25], and the temperature change is also small. Therefore, the density change during air flow in the main cable can be ignored, and other physical property parameters can also be regarded as constants for the same reason. In theoretical analysis and processing of experimental data, it is carried out according to common physical property problems.

During air flow in the main cable due to continuous absorption of water in the main cable participating fluid mass variable on different sections of main cable flow and heat and mass exchange affect each other increasing the complexity of the theory However according to data tested by Runyang Bridge and Humen Bridge fluid mass change in a main cable about 1% can be ignored [25]. Therefore, research does not need to couple flow and heat and mass exchange problems. Fluid flow resistance and heat and mass exchange can be treated separately.

4.2.1. Navier-Stokes Equation

In terms of size, the length of the suspension bridge main cable is in kilometers, and the diameter is generally about one meter. Its length is much larger than its diameter. According to fluid mechanics theory, it can be simplified into one-dimensional flow along the main cable direction. Then there is the Navier–Stokes equation [26] as follows:

$$F_z = \frac{1}{\rho}\frac{\partial p}{\partial z} + v\left(\frac{\partial^2 u_z}{\partial r^2} + \frac{1}{r}\frac{\partial u_z}{\partial r} + \frac{1}{r^2}\frac{\partial^2 u_z}{\partial \theta^2} + \frac{\partial^2 u_z}{\partial z^2}\right) \tag{3}$$

After simplification:

$$F_z = \frac{\partial u_z}{\partial t} + u_r\frac{\partial u_z}{\partial r} + \frac{\partial_\theta}{r}\frac{\partial u_z}{\partial \theta} + u_z\frac{\partial u_z}{\partial_z} \tag{4}$$

Use the Reynolds number calculation formula to judge the fluid flow state in the main cable:

$$\mathrm{Re} = \frac{\rho v L}{\mu} \tag{5}$$

where Re is Reynolds number, ρ is fluid density, μ is dynamic viscosity coefficient, v is flow field characteristic velocity, L is flow field feature length.

The internal gas of the main cable is regarded as air, and the characteristic velocity of the flow field is low, and the Reynolds number is small, and the flow state belongs to laminar flow. The complex flow can be regarded as flowing in a circular tube with an equivalent diameter of D [20], and the calculation formula for the equivalent diameter is as follows:

$$D = \frac{4A}{x} \tag{6}$$

where D is the equivalent diameter of the round tube, A is flow cross-sectional area, x is the wetted perimeter.

Then according to the theory of steady laminar flow in a laminar circular tube in fluid mechanics, calculate the velocity distribution on the axis of this equivalent diameter circular tube flow:

$$\mu_z = \frac{\gamma J}{4\mu}(R^2 - r^2) \tag{7}$$

where μ_z is axial flow rate, γ is specific weight, μ is dynamic viscosity, J is hydraulic slope, r is the distance from any point in the tube to the center of the circle.

Considering that the flow direction is approximately perpendicular to the direction of gravity (in actual operating suspension bridges, the main cable is a suspension line, and the fluid in it is gas), the influence of volume force is ignored and obtained:

$$\Delta p = rJl \tag{8}$$

where l is the length between the inlet clamp and the outlet clamp.

Substitute the general expression for hydraulic gradient into arrangement [27]:

$$\Delta p = \frac{1}{2}\lambda\frac{l\rho V^2}{D} \tag{9}$$

where V is average flow velocity, λ is the drag coefficient [19].

4.2.2. Triangular-like Pore

The shape of the pores in the main cable is formed by the accumulation of gaps arranged by the main cable steel wires. In most cases, the shape of the pores is a triangular structure formed by stacking three steel wires. In this case, it is assumed that the pores inside the main cable are triangular [21], and the total cross-sectional area of the triangular pores in the main cable is A, and the equivalent diameter is de, as shown in Figure 14.

Figure 14. Triangular-like pore.

When gas flows through the main cable, the airflow between the pores is interconnected. If we consider the mutual influence between the pores, then the calculation will become very complicated and difficult to predict. Here we assume that each pore is independent and the mutual influence between the pores is represented by an influence coefficient k. The pressure loss calculation formula per unit length is as follows [28]:

$$\Delta p = \lambda\frac{\Delta l v^2}{2gde}\gamma = Q\frac{32kv\gamma}{de^2 Ag} \tag{10}$$

where λ is pipe friction resistance coefficient, de is equivalent diameter, γ is the specific gravity of flowing matter, v is the velocity of flow, ν is kinematic viscosity, Δl is unit length.

The constant γ and ν vary with temperature, and the value at 20 °C is used here. The pressure loss in the pipeline is calculated as follows:

$$\Delta p = Q\frac{32kv\gamma}{{de_1}^2 A_1 g} \tag{11}$$

There will be a small amount of leakage of dry air during the flow process [29,30]. This flow process is difficult to observe and is affected by many unknown factors. According to the ideal flow process, the following assumptions are made: For a unit length of the main cable, the gas leakage is the same and the leakage rate is constant. The air volume entering the interior of the main cable is Q, and the gas volume leaked in each section is q_i, as shown in Figure 15.

Figure 15. Schematic diagram of gas leakage.

The pressure loss of the entire dehumidification section is obtained by adding up the pressure loss of each small section, but there will be a certain loss for every section length that the air flow enters, and the loss amount is q_i. The air flow loss will cause the pressure loss to decrease. At this time, the expression for the total pressure loss is:

$$\Delta p = Q\frac{32kv\gamma}{de_1{}^2 A_1 g}[1 + \sum_{i=1}^{n-1}(1-x)^i] \tag{12}$$

In the above formula, x is usually selected as different values according to the condition of the main cable protective layer as a gas leakage rate. The leakage rate of Runyang Bridge is 0.005, here we take three reference values: 0.01, 0.005, and 0.0000001.

4.2.3. Inlet Pressure

When the main cable dehumidification system is added to the Xihoumen Bridge, it will inevitably damage the outer wrapping structure of the main cable. Therefore, we have to make certain restrictions on inlet pressure. Pressure exceeding 2000 Pa may cause damage to the outer layer of the main cable [31]. The gas pressure discharged from the outlet of the dehumidifier is about 14,000 Pa. The pressure range when it is sent to each air clamp by pipeline is between 200~1000 Pa. The gas flow rate is between 4.0~11.5 m/s. It can be calculated that when the gas flows inside a main cable with a diameter of 855 mm, the pressure loss is between 200~300 Pa. To ensure dehumidification capacity, the inlet pressure should not be lower than 300 Pa.

4.3. Air Volume

4.3.1. Dehumidification Capacity

The temperature of the air after entering the main cable is about 20 degrees Celsius, here we take 20 degrees Celsius. At 100% relative humidity, its moisture content is 17.2 g/m^3. According to the design parameters of the dehumidifier, after passing through the dehumidifier, the moisture content of air is 6.2 g/m^3 and under a drying efficiency of 50%, each cubic meter of dry air passing through the interior of the main cable can take away 5.5 g of water.

4.3.2. Air Volume Selection

Air volume is the most important parameter in dehumidification system design [32]. Without considering main cable leakage, when the length of the main cable is fixed, estimating water content inside the main cable based on dry air moisture absorption capacity can derive air volume during the dehumidification cycle, which represents air volume required by the dehumidification system under ideal conditions to reduce humidity inside the main cable to the theoretical value, while under interference from external environment actually required air volume will differ from calculated value with calculation formula for air volume as follows:

$$Q = \frac{1000wl}{T \times 24 \times 60 \times \Delta_w} \tag{13}$$

where Q is Air volume, w is moisture content per unit length, l is length of the main cable, Δ_w is dehumidification capacity of 1 m^3 air, T is dehumidification time.

Considering leakage rate as x, the calculation formula for air volume becomes:

$$Q = \frac{1000w[1 - \frac{1}{(1-x)^l}]}{T \times \Delta_w \times 24 \times 60 \times (1-x)(1 - \frac{1}{1-x})} \tag{14}$$

where Q is Air volume, w is moisture content per unit length, l is the length of the main cable, Δ_w is dehumidification capacity of 1 m^3 air, T is dehumidification time, x is leakage rate.

Without considering leakage situation relationship between dehumidification time and air volume shown in Figure 16. Air volume for dehumidification system is greatly affected by pressure and size of air volume related to dehumidification time from the perspective of long-term stable anti-corrosion under determined inlet pressure water content and dehumidification capacity minimum air volume for Xihoumen Bridge main cable dehumidification system should be 30 m^3/h.

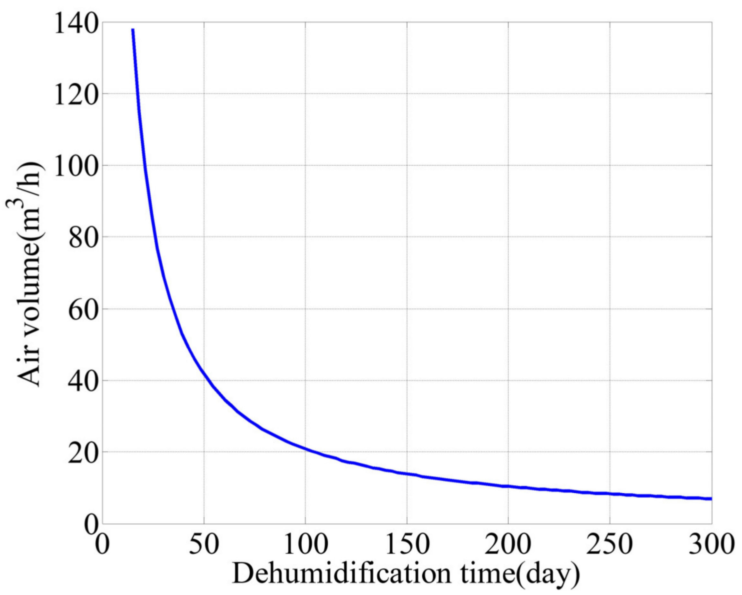

Figure 16. Relationship between dehumidification time and air volume.

4.4. Dehumidification Distance

The determination of the dehumidification distance largely relies on the results of the main cable ventilation experiment to select an empirical range. Currently, the dehumidification distance of most dehumidification systems is not less than 90 m and is between 150 and 200 m. This distance is more economical while ensuring a dehumidification effect. In the results of a single inlet and outlet experiment, when the dehumidification distance is above 200 m, the outlet effect is not ideal. Therefore, for the ventilation condition of the main cable of Xihoumen Bridge, the maximum dehumidification distance should not exceed 200 m and should be between 150 m and 180 m.

4.5. Dehumidification Time

During the dehumidification cycle when the dehumidification system is operating at full power, the time span may reach one year. During this period, the air conditions absorbed by the dehumidifier will also change. The absorbed air undergoes heating and condensation, and its relative humidity changes greatly due to temperature. If only considering removing water from inside the main cable and referring to previous data on water content inside the main cable, calculate the dehumidification time.

The gas flow rate through a certain section of the main cable is q_i, so the dehumidification time can be expressed as:

$$\Delta t_i = \frac{W}{q_i \Delta_w} \tag{15}$$

For a main cable section with a length of L, the calculation formula for dehumidification time is:

$$T = \int (\frac{W}{q_i \Delta_w}) dL \tag{16}$$

According to other parameters of dehumidification systems, draw a relationship between dehumidification distance and dehumidification time, where leakage rates are taken as 0.01, 0.005, and 0.0000001 respectively. As shown in Figure 17.

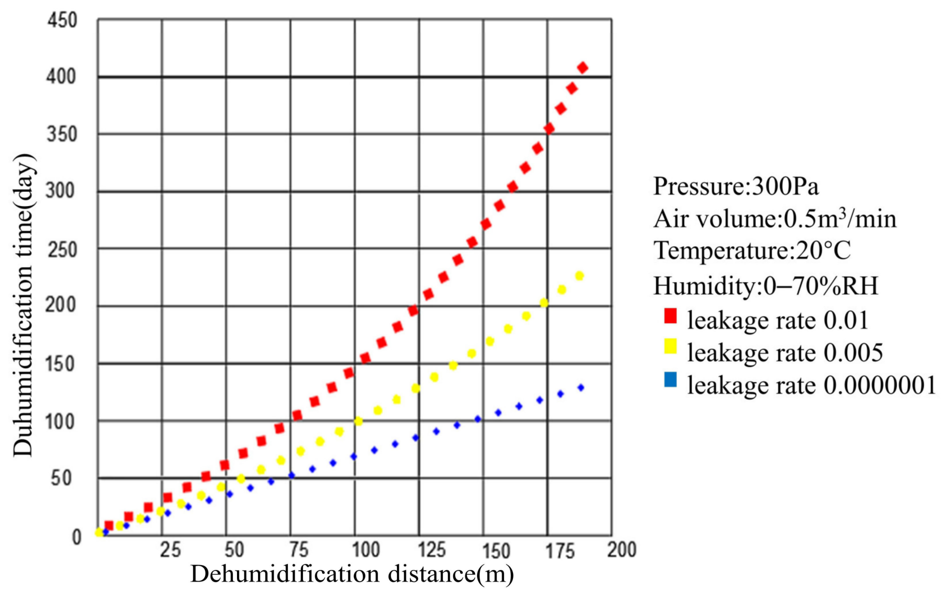

Figure 17. The dehumidification time varies with the dehumidification distance.

Dehumidification time is a dependent variable that is constrained by factors such as pressure, air volume, air humidity, leakage rate, dehumidification distance, and air humidity [33]. The range of values fluctuates greatly. The maximum value of the main cable dehumidification time is about 300 days and the minimum value is about 100 days.

4.6. Dehumidification Experiment

The dehumidification experiment was conducted with an air volume of 30 m^3/h and a pressure of 300 Pa. The dehumidification experiment was carried out by supplying gas from the No. 2 air clamp and outleting gas from the No. 0 air clamp. The dehumidifier was operated continuously during the ten-day experimental period, and data were collected every 60 min during the experiment period. The six sets of data were divided into one collection segment, and there were four collection segments per day (0 o'clock, 6 o'clock, 12 o'clock, and 18 o'clock). After organizing the data, it is shown in Figure 18.

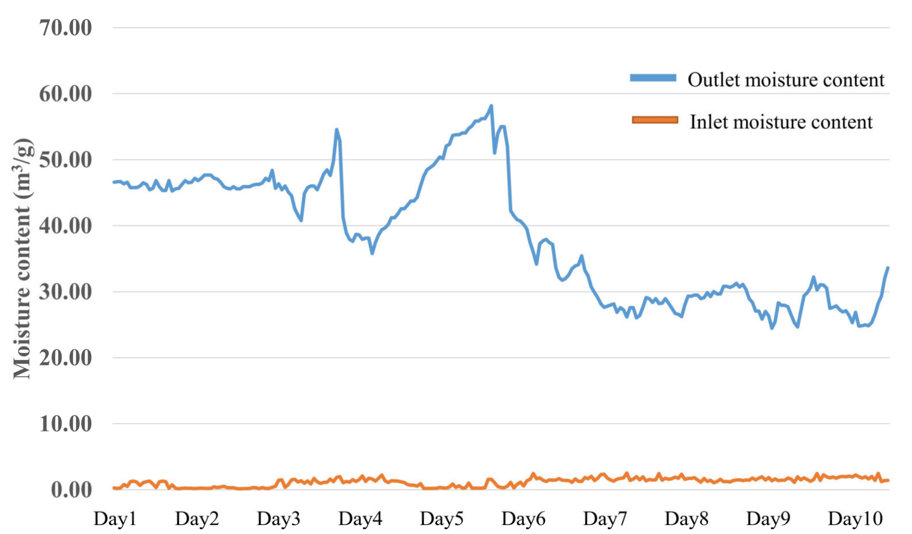

Figure 18. Dehumidification experiment moisture content changes.

The weather conditions during the ten-day dehumidification experiment are shown in Table 9.

Table 9. Weather for dehumidification experiments.

Date	Maximum Temperature	Minimum Temperature	Weather
1	6 °C	1 °C	cloudy
2	4 °C	0 °C	cloudy
3	4 °C	1 °C	cloudy
4	7 °C	3 °C	light rain
5	11 °C	2 °C	cloudy
6	10 °C	2 °C	sunny
7	7 °C	−1 °C	cloudy
8	11 °C	7 °C	cloudy
9	12 °C	4 °C	sunny
10	14 °C	4 °C	sunny

During the ten-day period, the dehumidification system operated normally, and the gas moisture content at the outlet clamp showed a continuous downward trend. Among them, there was a significant increase on the fourth day. Compared with local meteorological conditions, it can be inferred that the reason for the increase in moisture content was that it rained that day, which caused the internal of the main cable to be invaded by this external moisture, and humidity has a certain lag effect under the environmental influence. With the weather turning sunny in the next few days, the water content returned to a slow downward trend. The results of the dehumidification experiment are somewhat satisfactory, and under this parameter, the dehumidification system can achieve a basic dehumidification effect.

5. Conclusions

In this study, the design parameters of the dehumidification system were obtained by the main cable ventilation experiment. Using this set of parameters to conduct a dehumidification experiment, the result is that within ten days, the moisture content of the outlet clamp has dropped by about 37.5%, and the dehumidification capacity can meet the requirements. The conclusions are as follows:

(1) The water content inside the main cable is estimated to be 5.74 kg/m^3 based on the cross-sectional area and the number of steel wires of the main cable of the Xihoumen Bridge.
(2) In the ventilation experiment, it was found that when the air supply distance exceeds 200 m, it is difficult to detect the gas data at the outlet clamp, so the dehumidification distance should not exceed 200 m. This data agrees with that of other bridges.
(3) After experimental analysis, the resistance loss of the 150 m main cable is 200–300 Pa, so the air inlet pressure should not be lower than 300 Pa.
(4) Under the experimental conditions, the dehumidification capacity of the dehumidification system is 5.5 g/m^3. In order to achieve a good dehumidification effect, the air volume should be at least 30 m^3/h. Under single air inlet and double outltes, every 100% increase in air volume will increase the dehumidification capacity by 35%.
(5) Increase the number of outlet clamps to obtain a higher discharge ratio.
(6) The time for Xihoumen Bridge to complete a main cable dehumidification is estimated to be 100–300 days.

There are still some deficiencies in this study, which will be the focus of our future research:

(1) This experiment is carried out at the lowest point of the mid-span where the main cable is almost parallel to the ground, without considering the condition of the inclined part of the main cable.
(2) The time of the experiment is December local time, and the working time of the dehumidification system includes all the times of the year. That means the study ignored other climate conditions.

(3) Due to the inconsistent internal conditions of different main cables, the results of this study are not applicable to other main cables.

Author Contributions: Conceptualization, Z.G.; methodology, J.S.; validation, P.P., J.S. and W.S.; investigation, Z.G., W.S. and Q.L.; resources, J.S. and H.G.; data curation, P.P., W.S. and Q.L.; writing—original draft preparation, Z.G.; writing—review and editing, J.S.; project administration, H.G., J.S. and P.P. All authors have read and agreed to the published version of the manuscript.

Funding: This research received no external funding.

Data Availability Statement: The data supporting the findings of this study are available within the article.

Conflicts of Interest: The authors declare no conflict of interest.

References

1. Day, W. Telford's Menai and Conwy suspension bridges, Wales. In Proceedings of the Institution of Civil Engineers-Civil Engineering; Thomas Telford Ltd.: London, UK, 2007; pp. 26–30.
2. Fakhimi, R.; Shahabsafa, M.; Lei, W.; He, S.; Martins, J.R.; Terlaky, T.; Zuluaga, L.F. Discrete multi-load truss sizing optimization: Model analysis and computational experiments. *Optim. Eng.* **2022**, *23*, 1559–1585. [CrossRef]
3. Ghyabi, M.; Timber, L.C.; Jahangiri, G.; Lattanzi, D.; Shenton III, H.W.; Chajes, M.J.; Head, M.H. Vision-Based Measurements to Quantify Bridge Deformations. *J. Bridge Eng.* **2023**, *28*, 05022010. [CrossRef]
4. OGIHARA, K. Maintenance of Suspension Bridges: Cable Dehumidification. In *Inspection, Evaluation and Maintenance of Suspension Bridges*; CRC Press: Boca Raton, FL, USA, 2015; pp. 218–237.
5. Deeble Sloane, M.J.; Betti, R.; Marconi, G.; Hong, A.L.; Khazem, D. Experimental analysis of a nondestructive corrosion monitoring system for main cables of suspension bridges. *J. Bridge Eng.* **2013**, *18*, 653–662. [CrossRef]
6. Zhang, M.; Huang, S.; Li, P.; Shah, K.W.; Zhang, X. Application of dehumidification as anti-corrosion technology on suspension bridges: A review. *Appl. Therm. Eng.* **2021**, *199*, 117549. [CrossRef]
7. Suzumura, K.; Nakamura, S.-i. Environmental factors affecting corrosion of galvanized steel wires. *J. Mater. Civ. Eng.* **2004**, *16*, 1–7. [CrossRef]
8. Nakamura, S.; Suzumura, K. Experimental study on repair methods of corroded bridge cables. *J. Bridge Eng.* **2012**, *17*, 720–727. [CrossRef]
9. Jensen, J.L.; Lambertsen, J.; Zinck, M.; Stefansson, E. 16.10: Challenges with water ingress in bridge cable systems. *Ce/papers* **2017**, *1*, 4113–4122. [CrossRef]
10. Larsen, K.R.; Writer, S. Dry air combats corrosion on suspension bridge cables. *Mater. Perform.* **2008**, *47*, 30.
11. Furuya, K.; Kitagawa, M.; Nakamura, S.-i.; Suzumura, K. Corrosion mechanism and protection methods for suspension bridge cables. *Struct. Eng. Int.* **2000**, *10*, 189–193. [CrossRef]
12. Sampath, S.S.; Kumar, S.; Reddy, S.K. Influence of different desiccants, flow type and packings on the liquid desiccant dehumidification system: A review. *Int. J. Air-Cond. Refrig.* **2020**, *28*, 2030002. [CrossRef]
13. Guanzhong, P.; Xiaoping, M.; Daiyong, J.; Liangkai, F.; Chunyu, Z.; Luyan, S. Design research on dehumidification system for main cable of suspension bridge. *J. Shenzhen Univ. Sci. Eng.* **2013**, *30*, 179–185.
14. Gagnon, C.; Svensson, J. Suspension bridge cable evaluation and maintenance. In *IABSCE-JSCE Joint Conference on Advances in Bridge Engineering-II*; Ammann & Whitney: New York, NY, USA, 2010; pp. 567–575.
15. Chen, C. Latest research progress of main cable dehumidification system of suspension bridge in China. *Eng. Sci.* **2012**, *12*, 95–99.
16. Beabes, S.R.; Colford, B.R.; Bulmer, M.J. Dehumidification–An Effective Strategy for Preserving the Cables of Suspension Bridges. In Proceedings of the IABSE Symposium: Engineering the Future, Vancouver, BC, Canada, 21–23 September 2017; pp. 978–985.
17. Cao, P.; Fang, H.; Liu, W.; Zhuang, Y.; Fang, Y.; Li, C. Circumferential Expansion Property of Composite Wrapping System for Main Cable Protection of Suspension Bridge. *Adv. Polym. Technol.* **2020**, *2020*, 8638076. [CrossRef]
18. Chen, W.; Shen, R.; Que, M.; Gong, M.; Miao, R. New dehumidification system design and dehumidification test for the main cable of suspension bridge. *J. Civ. Struct. Health* **2021**, *11*, 1321–1335. [CrossRef]
19. Chen, W.; Shen, R.; Wan, T.; Ling, Q.; Wang, Z.; Zhou, Z. Pressure loss of internal dry air supply dehumidification system in main cable of suspension bridge. *J. Southeast Univ.* **2021**, *51*, 227–234.
20. Wei, Z.; Peng, F.; Miao, X.; Jia, D.; Zang, Z.; Wei, H. Numerical calculation and experiment on the dehumidification system for main cable of suspension bridge. *J. Eng. Thermophys.* **2016**, *37*, 2495–2501.
21. Jia, D.Y.; Sui, L.Y.; He, M.L. Experimental study on mass transfer coefficient of dry air in main cable of suspension bridge. In *Advanced Materials Research*; Trans Tech Publications Ltd.: Bäch, Switzerland, 2012; pp. 151–154.
22. Bloomstine, M.L.; Sørensen, O. Prevention of main cable corrosion by dehumidification. In *Advances in Cable-Supported Bridges*; CRC Press: Boca Raton, FL, USA, 2017; pp. 215–228.
23. Bloomstine, M.; Melén, J. Optimizing main cable dehumidification systems. In *Risk-Based Bridge Engineering*; CRC Press: Boca Raton, FL, USA, 2019; pp. 34–46.

24. Jensen, J.L.; Lambertsen, J.; Zinck, M.; Stefansson, E. Challenges of water ingress into bridge cable systems. *Steel Constr.* **2017**, *10*, 200–206. [CrossRef]
25. Li, H. Design and construction of dehumidification system for main cables of suspension bridge of Runyang bridge. *Bridge Constr.* **2005**, *1*, 39–44.
26. Chorin, A.J. Numerical solution of the Navier-Stokes equations. *Math. Comput.* **1968**, *22*, 745–762. [CrossRef]
27. Dai-yong, J.; Yin-kui, Y.; Xiaoping, M. Experiment Research of Dry Air Floating Resistance for Ventilation in the Cables of Suspension Bridge. *Fluid Mach.* **2003**, *31*, 9–11.
28. Tu, Z.; Peng, F.; Wei, Z.; Qian, G.; Wang, J.; Huang, C. *Simplified Calculation of Flow Resistance of Suspension Bridge Main Cable Dehumidification System*; Tech Science Press: Henderson, NV, USA, 2021.
29. Bloomstine, M. Latest developments in suspension bridge main cable dehumidification. In *Durability of Bridge Structures, Proceedings of the 7th New York City Bridge Conference, New York, NY, USA, 26–27 August 2013*; CRC Press: Boca Raton, FL, USA, 2013; p. 39.
30. Xue, D.; Liu, J.; Song, Y.; Zhang, X. Performance Analysis of a Hybrid Dehumidification System Adapted for Suspension Bridge Corrosion Protection: A Numerical Study. *Appl. Sci.* **2023**, *13*, 4219. [CrossRef]
31. Bloomstine, M. Main cable corrosion protection by dehumidification: Experience, optimization and new developments. In *Modern Techniques in Bridge Engineering, Proceedings of 6th New York City Bridge Conference, New York, NY, USA, 25–26 July 2011*; CRC Press: Boca Raton, FL, USA, 2011; p. 39.
32. Bloomstine, M.; Melén, J. Main cable dehumidification—Flow testing and other innovations. In *Asset Management of Bridges*; CRC Press: Boca Raton, FL, USA, 2017; pp. 13–28.
33. Chen, W.; Shen, R.; Wang, H.; Gong, W. Study of Anticorrosion System and Anticorrosion Mechanism for the Main Cable of Suspension Bridge. *J. Bridge Eng.* **2021**, *26*, 04021088. [CrossRef]